



‘Formability Analysis of Parabolic Cups drawn using Single Point Incremental Forming Process using AA7049’

P.Saiteja*, G. Devendar, A. Chennakesava Reddy

*PG student, Department of Mechanical Engineering, JNTUH UCESTH, India

Assistant Professor, Department of Mechanical Engineering, JNTUH UCESTH, India

Senior Professor, Department of Mechanical Engineering, JNTUH UCESTH, India

ABSTRACT

Single Point Incremental Forming (SPIF) emerges as a promising metal forming technique. SPIF involves localized deformation of a sheet blank using a simple spherical or hemispherical tool. This tool is affixed to a basic CNC machine equipped with three degrees of freedom (X, Y, and Z axes), allowing for precise tool movement along a predetermined path with vertical feed. This project discusses about the finite element analysis of single point incremental sheet forming (SPIF) process to form parabolic cups using aluminum alloy AA7049. ABAQUS 6.14 software code is used for finite element analysis. The process parameters of SPIF are maximum equivalent stress, strain, sheet thickness. Design of experiments was carried out as per Taguchi technique using L9 orthogonal array. ANOVA is done on the results of Taguchi trials.

KEYWORDS: Single point incremental forming process, AA7049, parabolic cup, tool radius, step depth, coefficient of friction.

INTRODUCTION

A method known as incremental deep drawing, or Incremental Sheet Forming (ISF), is employed to shape a metal sheet into the final work piece. This technique offers versatility, yielding high-quality production in a shorter timeframe and at a lower setup cost compared to other sheet forming processes. In incremental deep drawing, a metal sheet, free to move along the Z-axis, is clamped in the XY plane for the forming operation. A round-tipped tool, often attached to a CNC machine, gradually indents the sheet while following a predefined shape to create the desired portion. The tool moves in the XY plane, synchronized with Z-axis movements, to progressively shape the sheet. This process continues until the entire part is formed. MATLAB software is utilized to generate the component program, regulating the tool's path.

In a series of research on deep drawing process, a rich investigation have been carried out and

found majority of thickness reduction takes place in the walls of the cup but not in the flange or bottom of the cup [1], have found that the highest value of the forming angle results in the largest equivalent plastic strains on the sheet surface and larger thinning[2], process parameters which influence the formability of truncated pyramidal cups of AA1050-H18 alloy were coefficient of friction and tool radius [3], major parameter, which influences the effective stress, is the step depth 304 Stainless Steel[4].

This approach employs a Computer Numerically Controlled (CNC) machine to transform the metal sheet into the desired product. It stands out as an innovative method in metal forming, as it enables the creation of intricate exterior forms without the necessity of punches and dies. Particularly advantageous for rapid prototyping,

complex shapes can be achieved without the need for dies or punches.

To achieve the desired form, a round-headed tool applies localized pressure to shape the sheet metal blank. The CNC machine precisely controls the tool's path, sculpting designs through gradual movements. This method enhances the formability of sheet metal while ensuring a clean surface finish. Industries such as automotive, aerospace, medical, and packaging find applications for this advanced metal forming technique.

MATERIALS AND METHODS

Material Used

A popular aluminum alloy that is sometimes referred to as 7049 aluminum is AA7049. It belongs to the 7000 class of aluminum alloys, which are renowned for having a superb balance of strength, resistance to corrosion, and weld ability. The adaptable material AA7049 is utilized in many different applications, including aerospace and automotive parts as well as structural components.

All things considered, AA7049 is a common aluminum alloy that is utilized in numerous industrial and manufacturing applications due to its strength and adaptability.

Table 1: Chemical Composition of AA7049

Element	Al	Mg	Zn	Cu	Cr
Content (%)	88.7	2.5	7.6	1.5	0.15

Table 2: Mechanical properties of AA7049

Property	Value
Density	2840g/cubic mm
Young's Modulus	71.7GPa
Ultimate tensile strength	517MPa
Poisson's ratio	0.33

The tension test results for material AA7049 are used to calculate the true stress-true strain values. Figure displays the stress and strain graph for the AA7049 alloy. The values that were acquired used for calculation of effective plastic stress and effective plastic strain and the calculated values were used as the material characteristics in the Incremental deep drawing process simulation.

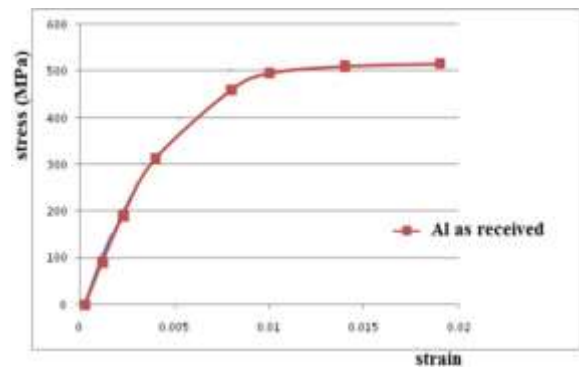


Figure 1: True stress-strain curve of AA7049

DESIGN OF EXPERIMENTS

Four adjustable process parameters were selected for Incremental deep drawing in the current work, and each process parameter was selected at three different levels. Table provides a summary of these process parameters together with their respective levels. When utilizing ABAQUS software for experimental and finite element analysis (FEA), the orthogonal array (OA), L9 was the favored choice.

Table 3: Process Parameters and levels

Factor	Symbol	Level 1	Level 2	Level 3
Sheet thickness(mm)	A	0.8	1	1.2
Step depth(mm)	B	0.5	0.75	1
Tool radius(mm)	C	4	6	8
Coefficient of friction	D	0.05	0.1	0.15

Table 4: Orthogonal array (L9) and control parameters

Trial No.	A	B	C	D
1	3	1	3	2
2	1	1	2	2
3	1	3	1	3
4	2	2	2	3
5	2	1	3	3
6	2	3	1	1
7	1	2	3	1
8	3	3	1	2
9	3	2	2	1

Finite Element Modeling and Boundary conditions

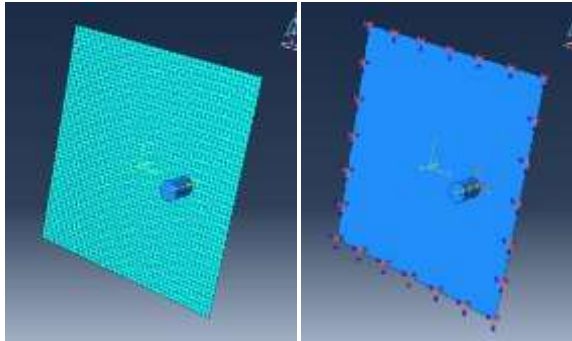


Figure 2: Meshed sheet and tool and boundary conditions.

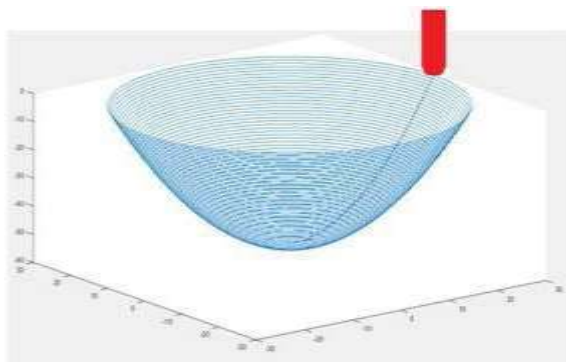


Figure 3: Tool path profile

RESULTS AND DISCUSSION

The controllable process variables were sheet thickness, tool radius, step depth, coefficient of friction.

Effect of process variables on effective stress

The effective stresses were respectively 252MPa, 411MPa, 218MPa, 220MPa, 216.2MPa, 263MPa, 248MPa, 221.6MPa, 220.9MPa for trails 1 to 9. The maximum effective stress is observed in the cup of trail 2. In every instance, the von Mises stress does not surpass the ultimate strength of the AA7049 alloy. Because the AA7049 alloy underwent enough plastic deformation, the Von Mises stress was sharply reduced at the bottom the final part to form of the parabola cup.

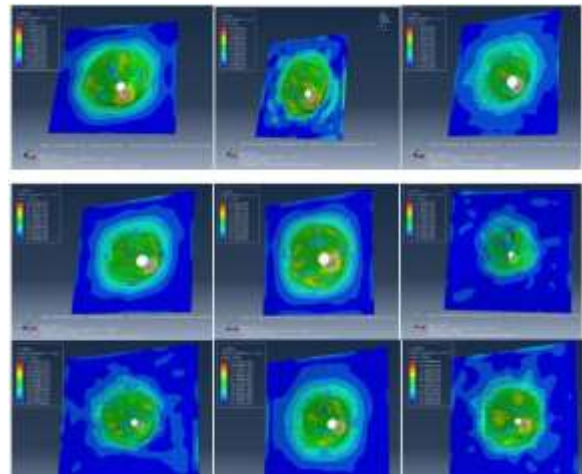


Figure 4: The von Mises stress induced in the parabola cups of all trail runs

The percentage contribution indicates that the parameter D, coefficient of friction, all by itself contributes 44.89%. The parameter sheet thickness (A) stands second and its influence is 25.21% on effective stress. The step depth (B) has an effect of 13.80% on the total variation in the effective stress. The tool radius (C) contributes 16.08% of the total variation in the effective stress.

Table 5: Analysis of Variance for Means

Source	DF	Seq SS	Adj SS	Adj MS	F	P	contribution
Sheet thickness	2	7787.6	7787.6	3893.78	*	*	25.21

Step depth	2	4261.6	4261.6	2130.78	*	*	13.80
Tool radius	2	4966.9	4966.9	2483.44	*	*	16.08
Coefficient of friction	2	13862.9	13862.9	6931.44	*	*	44.89
Total	8	30878.9	30878.9				100

Table 6: Response Table for Means

Level	Sheet thickness	Step depth	Tool radius	Coefficient of friction
1	293.7	240.0	245.3	307.3
2	233.0	282.7	283.7	219.7
3	229.7	233.7	227.3	229.3
Delta	64.0	49.0	56.3	87.7
Rank	2	4	3	1

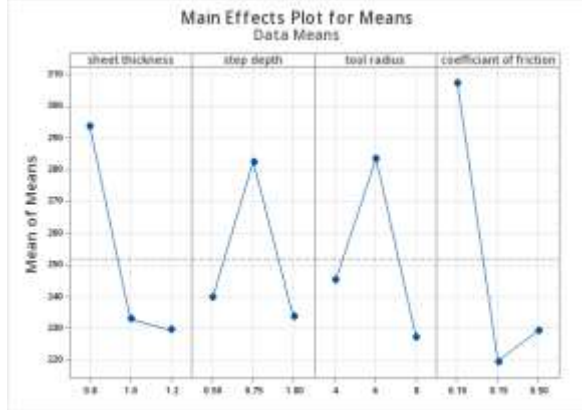


Figure 5: Effect of process parameters on von Mises stress

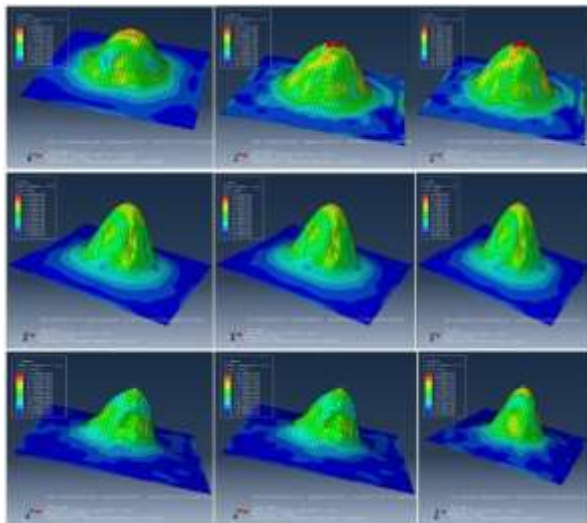


Figure 6: The von Mises stress induced in the paraboloid cups of all trail runs

Effect of process variables on Strain rate

The Figure 7 presents the effect of sheet thickness, step depth, tool radius, and coefficient of friction on strain rate induced in AA7049 sheet during incremental deep drawing. The strain rate was linearly increased with the sheet thickness. Greater thickness results in increased material available for plastic deformation. It is low for step depth of 0.5 mm. The strain rate was increased with the tool radius. The region under the tool that is subject to plastic deformation rises together with the tool radius. Therefore, a larger tool radius increases the strain rate. And the effect of coefficient of friction on strain rate was very minimal. The strain rates for trail 1 to 9 are 17.25, 20.02, 20.71, 20.05, 16.42, 23.18, 20.55, 25.74, and 21.52.

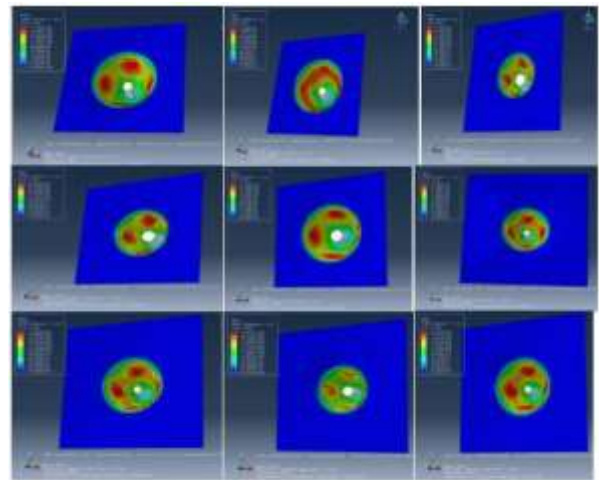


Figure 7: Strain rate induced in the paraboloid cups of all trail runs.

In Table 7, the percentage contribution indicates that the parameter D, coefficient of friction, all by itself contributes 36.65%. The parameter sheet thickness (A) stands second and its influence is 29.15% on effective strain. The step depth (B) has an effect of 15.16% on the total variation in the effective strain. The tool radius (C) contributes 19.02% of the total variation in the strain.

Table 7: Analysis of Variance for Means

Source	DF	Seq SS	Adj SS	Adj MS	F	P	contribution
Sheet thickness	2	18.4448	18.4448	9.2224	*	*	29.15
Step depth	2	9.5928	9.5928	4.7964	*	*	15.16
Tool radius	2	12.0383	12.0383	6.0191	*	*	19.02
Coefficient of friction	2	23.1947	23.1947	11.5973	*	*	36.65
Total	8	63.2706					100

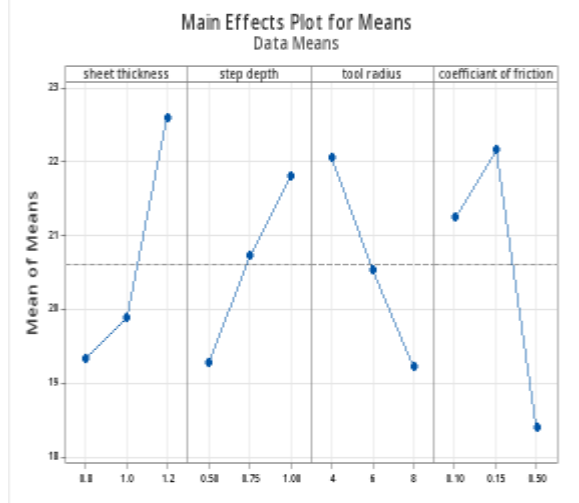


Figure 8: Effect of process parameters on strain

Table 8: Response Table for Means

Level	Sheet thickness	Step depth	Tool radius	Coefficient of friction
1	19.33	19.28	22.06	21.25
2	19.88	20.73	20.53	22.17
3	22.60	21.80	19.23	18.40
Delta	3.28	2.52	2.83	3.77
Rank	2	4	3	1

Effect of process variables on Thickness reduction

The figure 9 illustrates the impact of sheet thickness, step depth, tool radius, and coefficient of friction on the thickness reduction in AA7049 sheet during incremental deep drawing.

According to the data, thickness reduction increases with higher sheet thickness, step depth, and tool radius, while the coefficient of friction has a minimal effect. The thickness variation is primarily observed at the center-line of the deformed cup. Interestingly, most of the thickness reduction occurs in the walls of the cup rather than the bottom. The elements in the mid-region of the cup walls exhibit greater elongation compared to those at the bottom.

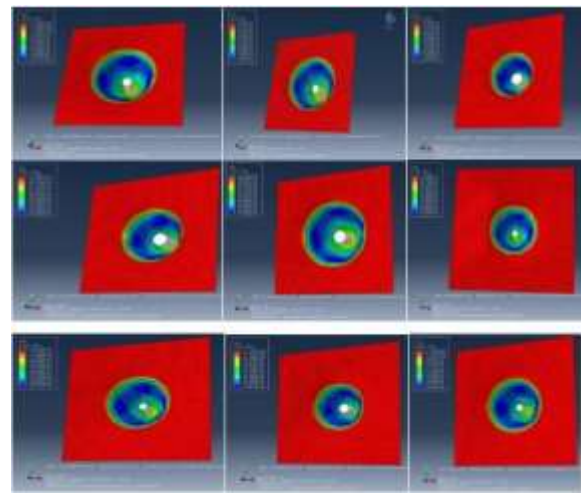


Figure 9: The reduction in thickness of the parabola cups of all trail runs

The sheet thickness stress values for trail 1 to 9 are 1.20, 8.00, 7.99, 9.99, 1.00, 9.99, 8.00, 1.20, and 1.20 shown in figure 9.

Table 9: Analysis of Variance for Means

Source	DF	Seq SS	Adj SS	Adj MS	F	P	contribution
Sheet thickness	2	19.156	19.156	9.578	*	*	14.09
Step depth	2	17.94	17.94	8.97	*	*	13.80
Tool radius	2	8.027	8.027	4.0133	*	*	0.05
Coefficient of friction	2	89.521	89.521	44.760	*	*	65.99
Total	8	134.644					100

Table 10: Response Table for Means

Level	Sheet thickness	Step depth	Tool radius	Coefficient of friction
1	5.730	6.397	4.130	1.133
2	6.993	3.400	6.397	8.663
3	3.467	6.393	5.663	6.393
Delta	3.527	2.997	2.267	7.530
Rank	2	3	4	1

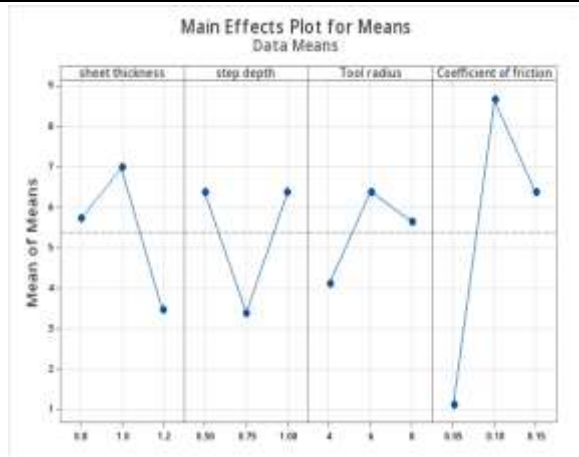


Figure 10: Effect of process parameters on sheet thickness

Analysis of this figure 11 reveals a notable trend: the primary thickness reduction occurs within the walls of the cup, with relatively minimal changes observed in the flange or bottom regions. Additionally, it's apparent that elements located in the midsections of the cup walls undergo greater elongation compared to those at the top and bottom. As depicted in the figure, there is a consistent reduction in thickness along the cup walls, while the bottom section experiences comparatively less change, and there is negligible alteration in the flange portion.

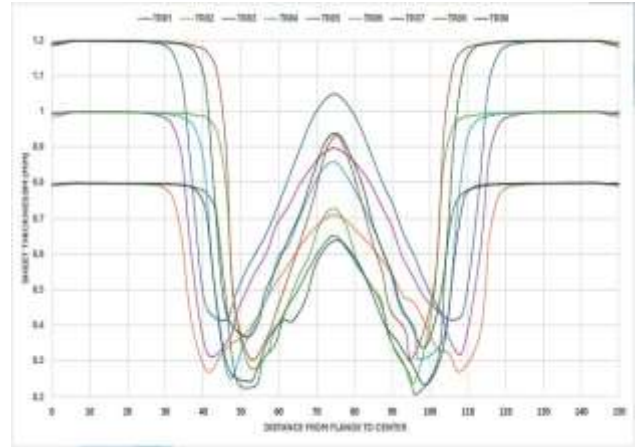


Figure 11: Location of thickness reduction in the deformed cup.

CONCLUSION

In this present work, the finite element analysis is successfully implemented to incremental deep drawing process for the AA7049 alloy sheet. Sheet thickness and Coefficient of friction is the major influencing parameter on the formability of Parabola cups of AA7049 alloy. The percentage contribution indicates that the parameter, coefficient of friction, all by itself contributes 44.89%. The parameter sheet thickness stands second and its influence is 25.21% on effective stress

The main factor influencing the effective stress for parabola cups made from AA7049 sheet is sheet thickness and the strain rate was linearly increased with the sheet thickness and is minimal at the flank.



REFERENCES

- [1] A. Chennakesava Reddy, Evaluation of Single Point Incremental Forming Process for Parabolic AA6082 Cups. *International Journal of Scientific & Engineering Research*, Volume 8, Issue 1, January-2017 964 ISSN 2229-5518
- [2] H. Arfa, R. Bahloul, H. Bel Hadj Salah Finite element modelling and experimental investigation of single point incremental forming process of aluminium sheets: influence of process parameters on punch force monitoring and on mechanical and geometrical quality of parts, *International Journal of Material Forming*, 2013.
- [3] V. Srija* and A. Chennakesava Reddy, Numerical Simulation of Truncated Pyramidal Cups Of Aa1050-h18 Alloy Fabricated By Single Point Incremental Forming, *International Journal Of Engineering Sciences & Research Technology* ISSN: 2277-9655 [June, 2016]
- [4] T. Santhosh Kumar, V. Srija, A. Ravi Teja, A. Chennakesava Reddy, Influence of Process Parameters of Single Point incremental Deep Drawing Process for Truncated Pyramidal Cups from 304 Stainless Steel using FEA, *International Journal of Scientific & Engineering Research*, Volume 7, Issue 6, June-2016 ISSN 2229-5518
- [5] L. Filice, L. Fratini, F. Micari, Analysis of material formability in incremental forming, *CIRP Ann Manuf Technol*, vol. 51, no. 1, pp. 199–202, 2002.
- [6] S. Thibaud, R. B. Hmida, F. Richard, P. Malecot, A fully parametric toolbox for the simulation of single point incremental sheet forming process: numerical feasibility and experimental validation, *Simulation Modeling Practice Theory*, vol. 29, pp. 42–43, 2012.
- [7] D.M Neto et.al. Evaluation of strain and stress states in the single point incremental forming process, *The International Journal of Advanced Manufacturing Technology*, vol. 85, page 521-534.31 0
- [8] Chennakesava Reddy, Finite element analysis of reverse superplastic blow forming of Ti-Al-4V alloy for optimized control of thickness variation using ABAQUS, *Journal of Manufacturing Engineering, National Engineering College*, vol. 1, no. 1, pp. 6-9, 2006.
- [9] A. C. Reddy, Parametric Significance of Warm Drawing Process for 2024T4 Aluminum Alloy through FEA, *International Journal of Science and Research*, vol. 4, no. 5, pp. 2345-2351, 2015.
- [10] A. C. Reddy, Formability of High Temperature and High Strain Rate Super-plastic Deep Drawing Process for AA2219 Cylindrical Cups, *International Journal of Advanced Research*, vol. 3, no. 10, pp. 1016-1024, 2015.
- [11] C. R Alavala, High temperature and high strain rate superplastic deep drawing process for AA2618 alloy cylindrical cups, *International Journal of Scientific Engineering and Applied Science*, vol. 2, no. 2, pp. 35-41, 2016.
- [12] C. R Alavala, Practicability of High Temperature and High Strain Rate Super-plastic Deep Drawing Process for AA3003 Alloy Cylindrical Cups, *International Journal of Engineering Inventions*, vol. 5, no. 3, pp. 16-23, 2016.
- [13] C. R Alavala, High temperature and high strain rate superplastic deep drawing process for AA5049 alloy cylindrical cups, *International Journal of Engineering Sciences & Research Technology*, vol. 5, no. 2, pp. 261-268, 2016.